Structural and Multidisciplinary Optimization (2019) 60:1921–1936
https://doi.org/10.1007/s00158-019-02300-z

RESEARCH PAPER

Optimized punch contact action related to control of local structure displacement

István Páczelt[1] · Zenon Mróz[2]

Received: 2 January 2019 / Revised: 4 April 2019 / Accepted: 2 May 2019 / Published online: 24 June 2019

Abstract
For a structure under service loads, there is a need to induce precise control of a local displacement by additional punch loading. Such problem exists in design of robot grippers or agricultural tools used in mechanical processing. The punch interaction is assumed to be executed by a discrete set of pins or by a continuously distributed contact pressure. The optimal contact force or pressure distribution and contact shape are specified for both discrete and continuous punch action. Several boundary support conditions are discussed, and their effects on punch action are presented.

Keywords Contact problem · Displacement control · Optimal pressure distribution · Optimal contact shape

1 Introduction

The structural optimization problems are usually related to specification of material parameters, size, shape, or topological variables, loading distribution, supports, element connections, etc. The required stiffness and strength levels are usually imposed as design constraints and the objective function assumed as the volume or cost of materials used, cf. recent books by Banichuk and Neittaanmaki (2010) or Banichuk (2011). A special class of contact optimization problems is characterized by searching for optimal contact traction distribution satisfying strength conditions at the contact interface. The review of contact optimization problems has been presented by Páczelt et al. (2016).

In the paper by Li et al. (2003), the evolutionary structural optimization (ESO) concepts have been applied with a non-gradient procedure presented for incremental shape redesign of contact interfaces. In Zabaras et al.'s (2000) work, a continuum sensitivity analysis has been presented for large inelastic deformations and metal-forming processes.

Responsible Editor: Somanath Nagendra

✉ István Páczelt
paczelt@freemail.hu

[1] University of Miskolc, H-3515 Miskolc-Egyetemváros, Hungary

[2] Institute of Fundamental Technological Research, Warsaw, Poland

In the papers by Páczelt and Szabó (1994), Páczelt (2000), Páczelt and Baksa (2002), and Páczelt et al. (2007), the method of contact shape optimization was developed for 2D and 3D problems with the objective to minimize the maximal contact pressure under specified loading conditions. The contact optimization problems for elements in the relative sliding motion with account for wear require special analysis referred to a steady-state wear process. The optimal design objective is to specify the contact shape minimizing the wear rate in the steady-state condition for progressive or periodic sliding. The extensive review of this class of problems has been presented by Páczelt et al. (2015). The monographs of Goryacheva (1998) and Wriggers (2002) provide a solid foundation for analytical and numerical methods of solution of contact problems, including wear analysis. The finite element analysis is most frequently applied in solving contact problems, cf. Szabó and Babuska (1991).

The present paper is devoted to a problem of local displacement control in a structure subjected to service loads, such as an assembling robot gripper (Monkman et al. 2006). Then the precise displacement value should be achieved at the location of robot interaction with an assembled element. It means that the displacement control should be applied at a point transmitting the interaction load. The method of solution of this new class of contact design problems will be discussed in Sect. 2 for the case of beam deflection control with the constraint set on maximal contact pressure. In Sect. 3, the specific examples are discussed, illustrating designs of punch shape for differing beam support constraints. In Sect. 4, the optimal contact

pressure distribution and punch shape are determined from the optimization procedure. Applying the strength constraint also punch position and contact zone size can be properly selected. The method presented can be extended to the analysis and design of optimal punch interaction aimed at displacement control at the loaded boundary point of any structural element.

2 Control of beam deflection at the loading point Q for differing support conditions

In the assembling process of mechanical elements conducted by a robot gripper, a typical operation is to place one body (cylinder) into a hole of another body. In this case, the cylinder must execute translation u_n^* under increasing axial force. In Fig. 1a, the force F_Q is equal to friction force at the interface between cylinder and hole. Another operation called "pick and place" is related to lifting the cylinder and placing in a new position, Fig. 1b. In this case, the cylinder is compressed along its diameter by two plates inducing normal contact displacements u_n^* non-linearly related to contact forces F_Q, assuring due to friction a fixed cylinder position relative to plates. In both operations, the prescribed force and displacement values are required at the same point.

Consider a cantilever beam built-in at its end A and loaded at point Q by the force F_Q, Fig. 2, inducing the deflection $u_n^{(2)}$. To keep the deflection of Q at the required value u_n^*, the discrete or continuous punch action is applied within the specified contact zone region Ω defined as an interval $L_1 \le x \le L_4$ and the contact center position $x = x_0$. The punch is allowed to translate in the normal direction $\boldsymbol{n}$ to the beam exerting contact pressure $p_n(x)$. The desired punch action occurs when the value of punch load F_0 is reached for the contact pressure distribution not exceeding the specified level $p_{\max}$. The value of F_0 depends on the size and position of the contact zone. The minimal value of F_0 is reached, when the concentrated load acts at $x = L_4$, but when the constraint $p_n \le p_{\max}$ is applied, then the constant pressure zone $p_n = p_{\max}$ at the boundary $x = L_4$ constitutes the optimal distribution. In our design, the location of the punch and the control function $c(x)$ are prescribed in advance and the value of $p_{\max}$ is controlled by the length of contact zone. The prescribed pressure distribution $p_n = c(x)\, p_{\max}$ is reached by determination of the initial gap between the punch and beam. The problem is solved in two main steps. First, using the stamp equilibrium condition at a given control function $c(x)$ and constraint of normal displacement at the point Q, the value of $p_{\max}$ is specified, see (6). Second, from contact condition between the stamp and beam, the initial gap between the contacting bodies is determined, see Appendix 1.

The constraint set on the maximal pressure value can be attained by assuming the following distribution in the contact zone specified by the control function

$$p_n = c(x)\, p_{\max}, \quad c(x) \le 1, \quad \text{for } x \in \Omega \tag{1}$$

Further, for technical reasons, it is assumed that the contact pressure distribution is symmetric with respect to center point of contact zone. This allows for punch application in differing support conditions.

Then obviously, the optimal distribution would correspond to $c(x) = 1$ and constant pressure $p_n = p_{\max}$; next, this value could be minimized. Figure 3 presents the assumed symmetric pressure distribution for different control functions. Using Hermite functions, two pressure distributions are specified. The formulae of Hermite functions are stated in the caption of Fig. 3.

Assuming the pressure distributions according to Fig. 3, the problem is reduced to specification of contact surface form

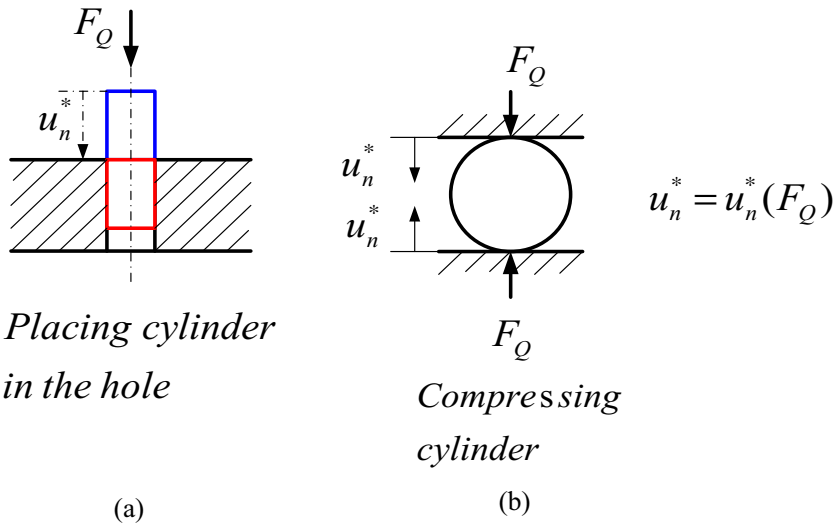

Fig. 1 Typical robot gripper operations: **a** placing cylinder into an element hole and **b** compressing cylinder by required normal forces

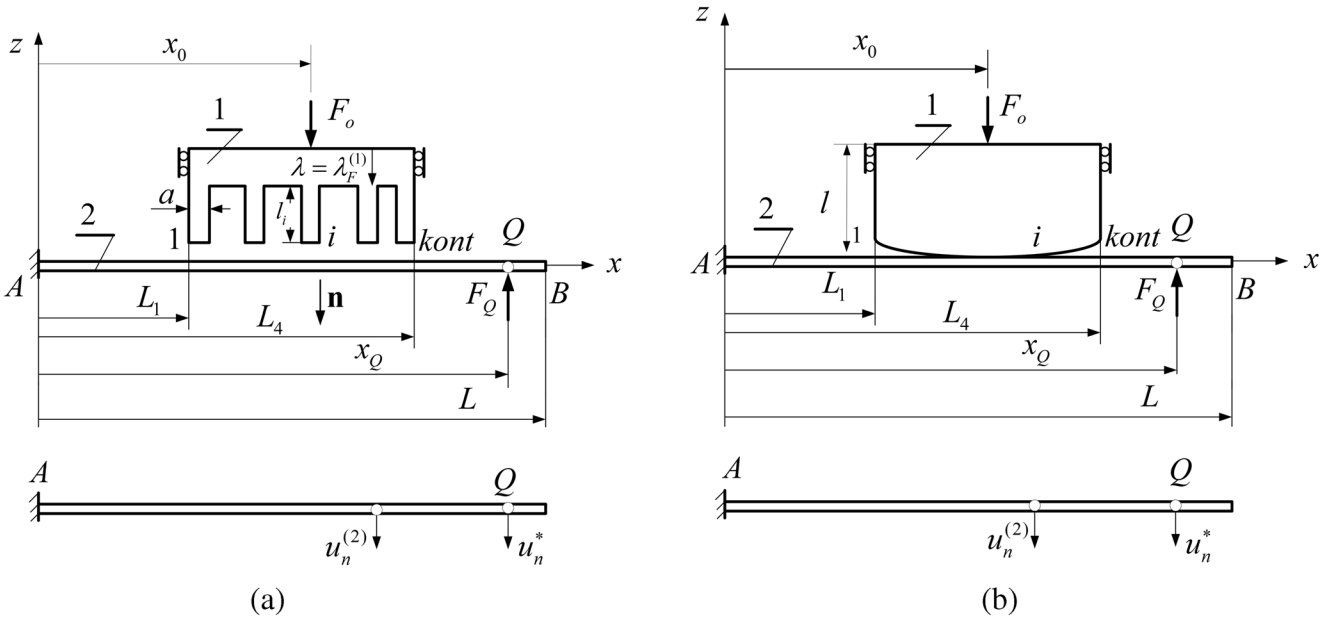

Fig. 2 Beam system for transmission of the punch load F_0 to maintain the vertical displacement u_n^* at the point Q loaded by the force F_Q; **a** discrete action by a set of pins and **b** continuous punch action

represented by the gap function. Several variants of this problem are treated and will be discussed in more detail.

The punch center position x_0 can be located on both sides of point Q. Depending on the support constraint, it can essentially affect the value of the required punch load F_0 or the deformation form. The effects of punch position will be discussed in Sect. 4.

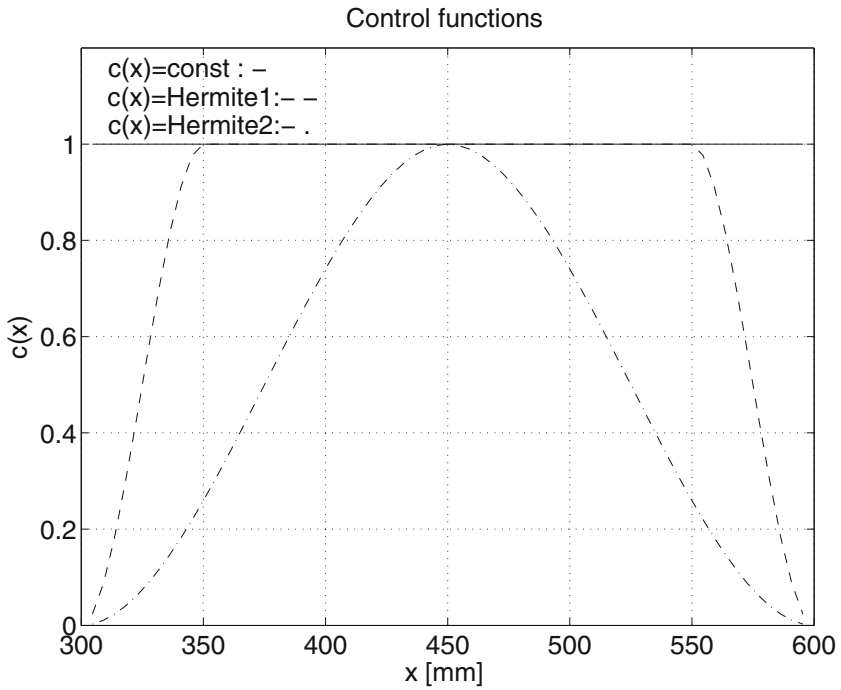

Fig. 3 Control function $c(x)$ for symmetric contact pressure distribution; for constant pressure: $c(x) = const = 1$; for Hermite 1: $L_1 = 300$, $L_2 = 350$, $L_3 = 550$, $L_4 = 600$, $c(x) = 0, \quad 0 \le x \le L_1; \quad c(x) = \left\{ 3\left(\frac{x-L_1}{L_2-L_1}\right)^2 - 2\left(\frac{x-L_1}{L_2-L_1}\right)^3 \right\}, L_1 \le x \le L_2; c(x) = 1, L_2 \le x \le L_3 \quad c(x) = \left\{ 1-3\left(\frac{x-L_3}{L_4-L_3}\right)^2 + 2\left(\frac{x-L_3}{L_4-L_3}\right)^3 \right\}, L_1 \le x \le L_4; c(x) = 0, L_4 \le x$; for Hermite 2: $L_1 = 300$, $L_2 = L_3 = 450$, $L_4 = 600$

2.1 Beam structure deflection control for different support conditions

2.1.1 First variant: cantilever beam built-in at the end a

Consider first the case of punch action executed by a set of punch pins, as shown in Fig. 2a, of thickness a, width b, and cross-section area $A = ab$. The forces between punch and beam are specified by (1), thus

$$P_j = Ac(x_j)p_{\max}, j = 1, 2, \ldots, kont \tag{2}$$

Under applied load F_0 on the punch, the maximal pressure results from the equilibrium condition

$$p_{\max} = \frac{F_0}{\sum_{j=1}^{kont} c(x_j) A} \tag{3}$$

Using the influence Green function $H^{(2)}(x, s)$, the beam displacement in the normal direction $\boldsymbol{n}$ along the z-axis equals

$$u_n^* = \sum_{j=1}^{kont} H^{(2)}(x_Q, x_j) P_J + u_{n,load}^{(2)} \tag{4}$$

where $u_{n,load}^{(2)} < 0$ is the displacement at point Q induced by the load F_Q. Using the influence function for calculation $u_{n,load}^{(2)}$, we can write $u_{n,load}^{(2)} = -H^{(2)}(x_Q, x_Q) F_Q = -H_{Q,Q}^{(2)} F_Q$. The influence function is defined in Appendix 3. In view of (4), there is

$$u_n^* = \sum_{j=1}^{kont} H^{(2)}(x_Q, x_j) c(x_j) A p_{\max} + u_{n,load}^{(2)} \tag{5}$$

and

$$p_{\max} = \frac{u_n^* - u_{n,load}^{(2)}}{\sum_{j=1}^{kont} H^{(2)}(x_Q, x_j) c(x_j) A} \tag{6}$$

Having specified $p_{\max}$, the punch pin height or punch contact shape can be determined.

The unilateral Signorini contact condition takes the form

$$d = \left(u_n^{(2)}(p_n) + u_{n,load}^{(2)}\right) - \left(u_n^{(1)}(p_n) + \lambda\right) + g^{(0)} \geq 0, p_n \geq 0, \quad p_n d = 0 \tag{7}$$

where $u_n^{(i)}(p_n) = \int_{S_c} H^{(i)}(x, s) p_n(s)\, ds$ is the normal displacement of beam or punch induced by the contact pressure, $H^{(i)}(x, s)$ is the Green function for normal displacements, $u_{n,load}^{(2)}$ is the normal displacement resulted from the load F_Q, $g^{(0)}$ is the initial gap, λ is the rigid body displacement of the punch, that is $d = d(p_n, \lambda)$, where the notation $\lambda_F^{(1)} = \lambda$ is used.

Usually, the contact problem is solved by the principle of modified complementary energy or by the displacement formulation using minimum principle of the total potential energy in the penalty form (cf. Wriggers 2002), (Konyukhov and Schweizerhof (2013). In the last case, we use p-versions of finite element method for discretization (cf. Szabó and Babuska 1991).

In these contact optimization problems, the initial gap (shape form of the contact surface) is the unknown function. In our case, the contact condition will be checked up at the *kont* points. Supposing contact at each check point, the calculation of the gap can be executed in terms of the special iterative procedure (Páczelt 2000; Páczelt et al. 2016) In Appendices 1 and 2, the discretized equations for determination of the initial gap between the beam and punch are provided.

2.1.2 Second variant: beam allowed to execute displacement along the sliding support A

Let us now refer to the system of Fig. 4, where beam 2 can execute the rigid body displacement $-u_{A,z} = \lambda_F^{(2)}$ along the sliding support A and deform elastically due to load F_Q and punch force F_0 action. Assume the initial beam configuration to correspond to contact engagement at Q with an object (e.g., cylinder).The vertical displacement at the point Q then is

$$u_n^* = u_n^{(2)} = \lambda_F^{(2)} + \sum_{j=1}^{kont} H^{(2)}(x_Q, x_j) P_J + u_{n,load}^{(2)} \tag{8}$$

Assuming that there is no force acting at the sliding support A, the equilibrium condition of beam 2 requires that

$$F_0 = F_Q, and\, p_{\max} = \frac{F_Q}{\sum_{j=1}^{kont} c(x_j) A} \tag{9}$$

as the contact forces are $P_j = Ac(x_j)p_{\max}$.

Using the influence function for calculation of $u_{n,load}^{(2)}$, we can write

$$u_{n,load}^{(2)} = -H^{(2)}(x_Q, x_Q) F_Q = -H_{Q,Q}^{(2)} F_Q \tag{10}$$

and the support displacement can be determined from Eq.(8)

$$\lambda_F^{(2)} = u_n^* - \left(\sum_{j=1}^{kont} H^{(2)}(x_Q, x_j) \frac{c(x_j)}{\sum_{k=1}^{kont} c(x_k)} - H_{Q,Q}^{(2)} \right) F_Q \tag{11}$$

The contact condition between the punch and beam is

$$u_{in}^{(2)} - u_{in}^{(1)} + g_i^{(0)} = 0, i = 1, \ldots, kont \tag{12}$$

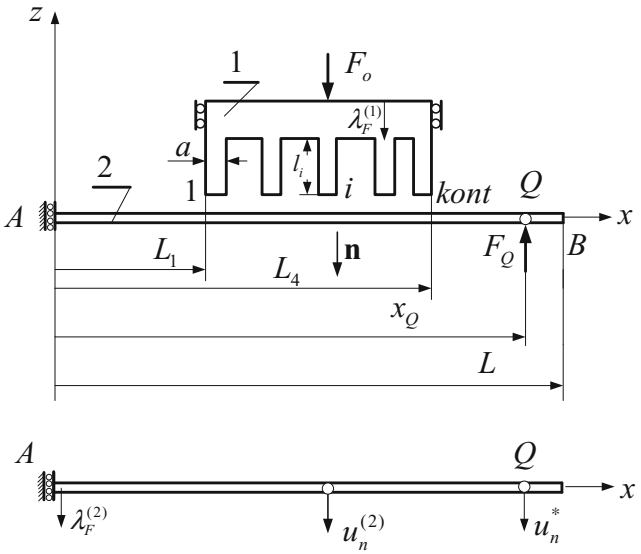

Fig. 4 Beam and punch system for transmission of load F_0 interacting with the force F_Q to induce vertical displacement u_n^*. Beam 2 is allowed for rigid body displacement $\lambda_F^{(2)}$ and elastic deformation

Using (62a), (12) can be expressed as follows

$$\lambda_F^{(2)} + \left(\sum_{j=1}^{kont} \left(H^{(1)}(x_i, x_j) + H^{(2)}(x_i, x_j) \right) \frac{c(x_j)}{\sum_{k=1}^{kont} c(x_k)} - H_{i,Q}^{(2)} \right) F_Q - \lambda_F^{(1)} + g_i^{(0)} = 0 \quad (13)$$

or

$$\lambda_F^{(2)} + \left(\sum_{j=1}^{kont} H(x_i, x_j) - H_{i,Q}^{(2)} \right) F_Q - \lambda_F^{(1)} + g_i^{(0)} = 0 \quad (14)$$

where

$$H(x_i, x_j) = \left(H^{(1)}(x_i, x_j) + H^{(2)}(x_i, x_j) \right) \frac{c(x_j)}{\sum_{k=1}^{kont} c(x_k)} \quad (15)$$

Discretizing (12)–(15), we can write

$$\mathbf{d} = \left({}^{iter}\mathbf{He} - \mathbf{h}_Q^{(2)} \right) F_Q + \mathbf{e}\lambda_F^{(2)} - \mathbf{e}\,{}^{(iter)}\lambda_F^{(1)} + {}^{(iter)}\mathbf{g}^{(0)} = \mathbf{0} \quad (16)$$

where

$\mathbf{h}_Q^{(2),T} = \left[H_{1,Q}^{(2)}, H_{2,Q}^{(2)}, \ldots, H_{i,Q}^{(2)}, \ldots, H_{kont,Q}^{(2)} \right]$, $\mathbf{e}$, see (63),

Because F_Q and $\lambda_F^{(2)}$ are known (see (11)), then ${}^{iter}\mathbf{u}$ can be calculated, namely

$${}^{iter}\mathbf{u} = \left({}^{iter}\mathbf{He} - \mathbf{h}_Q^{(2)} \right) F_Q + \mathbf{e}\lambda_F^{(2)} \quad (17)$$

and from the following equation

$${}^{iter}\mathbf{u} - \mathbf{e}\,{}^{(iter)}\lambda_F^{(1)} + {}^{(iter)}\mathbf{g}^{(0)} = \mathbf{0} \quad (18)$$

one can easily find ${}^{iter}\lambda_F^{(1)}$, ${}^{(iter)}\mathbf{g}^{(0)}$ supposing ${}^{(iter)}g_1{}^{(0)} = 0$. Then ${}^{(iter)}\lambda_F^{(1)} = {}^{(iter)}u_1$.

2.1.3 Third variant: free beam is allowed for rigid body translation and rotation

Referring to Fig. 5, consider the case, when the beam 2 is not constrained and is allowed for a rigid body vertical displacement $\lambda_F^{(2)}$ and rotation $\lambda_M^{(2)}$ at the beam end A. The displacement control is now required at two points Q_1 and Q_2, where the loads F_{Q_1} and F_{Q_2} are applied. The initial beam configuration corresponds to simultaneous contact engagement with interacting objects at Q_1 and Q_2.

The vertical displacement at point Q_s is

$$u_{sn}^* = u_{sn}^{(2)} = \lambda_F^{(2)} + \lambda_M^{(2)} x_{Q_s} + \sum_{j=1}^{kont} H^{(2)}(x_{Q_s}, x_j) P_J + u_{sn,load}^{(2)} \quad s = 1, 2 \quad (19)$$

Using the influence functions for calculation $u_{sn,load}^{(2)}$, we can write

$$u_{sn,load}^{(2)} = -\sum_{p=1}^{2} H_{Q_s,Q_p}^{(2)} F_{Q_p} \quad (20)$$

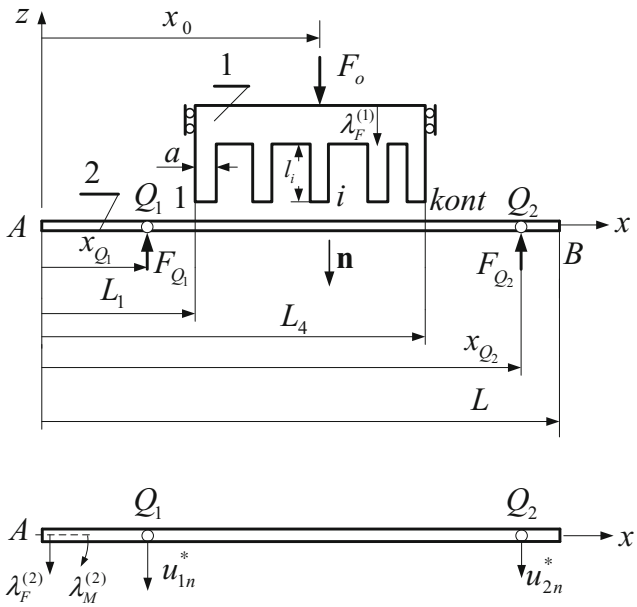

Fig. 5 Beam system for transmission of the load F_0 interacting with the forces F_{Q_1} and F_{Q_2} to induce vertical displacements u_{1n}^* and u_{2n}^*, when the beam 2 is allowed for rigid body translation $\lambda_F^{(2)}$ and rotation $\lambda_M^{(2)}$

From the force and moment equilibrium equations of the beam, we have

$$F_0 = F_{Q_1} + F_{Q_2} \quad 0 = x_0 F_0 - x_{Q1} F_{Q_1} - x_{Q_2} F_{Q_2} \tag{21}$$

and the position of control force F_0 is equal to

$$x_0 = \frac{x_{Q_1} F_{Q_1} + x_{Q_2} F_{Q_2}}{F_{Q_1} + F_{Q_2}}$$

Introducing the parameter $0 \le \zeta \le 1$ and defining the force $F_{Q_2} = (1-\zeta) F_{Q_1}$, the position of F_0 is

$$x_0 = \frac{x_{Q1} + x_{Q_2}(1-\zeta)}{2-\zeta} \tag{22}$$

when $\zeta = 0$, the forces $F_{Q_1} = F_{Q_2}$ and $x_0 = \frac{x_{Q1}+x_{Q_2}}{2}$, when $\zeta = 1$, then $F_{Q_2} = 0$ and $x_0 = x_{Q_1}$.

From the equilibrium equation for punch (3), the maximal contact pressure and the contact forces are

$$p_{\max} = \frac{F_0}{\sum\limits_{j=1}^{kont} c(x_j) A} \tag{23}$$

For derivation of the rigid body displacements, we have the following two equations

$$\lambda_F^{(2)} + \lambda_M^{(2)} x_{Q_s} = u_{sn}^* - \left(\sum_{j=1}^{kont} H^{(2)}(x_{Q_s}, x_j) \frac{c(x_j)}{\sum\limits_{k=1}^{kont} c(x_k)} F_0 - \sum_{p=1}^{2} H_{Q_s,Q_p}^{(2)} F_{Q_p} \right), s = 1,2 \tag{24}$$

The contact condition between the punch and beam is

$$u_{in}^{(2)} - u_{in}^{(1)} + g_i^{(0)} = 0, i = 1, \ldots, kont \tag{25}$$

and it can be expressed in the following form

$$\lambda_F^{(2)} + \lambda_M^{(2)} x_i + \left(\sum_{j=1}^{kont} H^{(2)}(x_i, x_j) \frac{c(x_j)}{\sum\limits_{k=1}^{kont} c(x_k)} F_0 - \sum_{p=1}^{2} H_{i,Q_p}^{(2)} F_{Q_p} \right) - \left(\lambda_F^{(1)} - \sum_{j=1}^{kont} H^{(1)}(x_i, x_j) \frac{c(x_j)}{\sum\limits_{k=1}^{kont} c(x_k)} F_0 \right) + g_i^{(0)} = 0 \tag{26}$$

or

$$\lambda_F^{(2)} + \lambda_M^{(2)} x_i + \left(\sum_{j=1}^{kont} H(x_i, x_j) F_0 - \sum_{p=1}^{2} H_{i,Q_p}^{(2)} F_{Q_p} \right) - \lambda_F^{(1)} + g_i^{(0)} = 0 \tag{27}$$

where

$$H(x_i, x_j) = \left(H^{(1)}(x_i, x_j) + H^{(2)}(x_i, x_j) \right) \frac{c(x_j)}{\sum\limits_{k=1}^{kont} c(x_k)} \tag{28}$$

Discretizing (26)–(28), we can write

$$\mathbf{d} = {}^{iter}\mathbf{H}\mathbf{e} F_0 + \sum_{p=1}^{2} \mathbf{h}_{Q_p}{}^{(2)} F_{Q_p} + \mathbf{e}\lambda_F^{(2)} + \mathbf{x}\lambda_M^{(2)} - \mathbf{e}^{(iter)} \lambda_F^{(1)} + {}^{(iter)}\mathbf{g}^{(0)} = \mathbf{0} \tag{29}$$

where.

$\mathbf{h}_{Q_s}^{(2),T} = \left(H_{1,Q_s}^{(2)}, H_{2,Q_s}^{(2)}, \ldots, H_{i,Q_s}^{(2)}, \ldots, H_{iter,Q_s}^{(2)} \right)$, s = 1, 2, $\mathbf{x}^T = [x_1, x_2, \ldots, x_i, \ldots, x_{kont}]$.

Because F_0 and F_{Q_p} $p = 1, 2$ and $\lambda_F^{(2)}$ and $\lambda_M^{(2)}$ are known, ${}^{iter}\mathbf{u}$ can be calculated from the equation

$${}^{iter}\mathbf{u} = \left({}^{iter}\mathbf{H}\mathbf{e} F_0 + \sum_{p=1}^{2} \mathbf{h}_{Q_p}^{(2)} F_{Q_p} \right) + \mathbf{e}\lambda_F^{(2)} + \mathbf{x}\lambda_M^{(2)} \tag{30}$$

and from the following equation

$$\mathbf{d} = {}^{iter}\mathbf{u} - \mathbf{e}^{(iter)} \lambda_F^{(1)} + {}^{(iter)}\mathbf{g}^{(0)} = \mathbf{0} \tag{31}$$

one can easily find ${}^{iter}\lambda_F^{(1)}$, ${}^{(iter)}\mathbf{g}^{(0)}$ supposing ${}^{(iter)}g_1{}^{(0)} = 0$. Then ${}^{(iter)}\lambda_F^{(1)} = {}^{(iter)}u_1$.

3 Numerical examples

The beam area $A_b = a_b h_b = 20 \cdot 50 = 1000\, mm^2$, inertia moment $I = a_b h_b^3/12 = 21833.33\, mm^4$, Young modulus $E = 2 \cdot 10^5\, MPa$ are assumed and other geometric parameters are:

$L_1 = 300$, $L_4 = 600$, $x_Q = 850$, $L = 900\, mm$. The punch centre position $x_0 = 450\, mm$ corresponds to the position parameter $\xi = x_0/x_Q = 0.529$. The specified vertical displacement at the point Q is $u_n^* = 1\, mm$, and the required force values are $F_Q = 4\, kN$, $F_Q = 5\, kN$, and $F_Q = 6\, kN$.

3.1 Example of the first variant

3.1.1 Discrete model

The punch contact executed by five punch pins of crosssection area $A = aa_b = 5 \cdot 20 = 100\, mm^2$ (Fig. 2a). The x coordinates of the punch pins are: 383.33, 416.66, 450.00, 483.33, and 516.66 mm.

The beam deflection is presented in Fig. 6a for three control functions and $F_Q = 5\, kN$. It is seen that their effect is very

small. The biggest displacement corresponds to the Hermite 2 control function (see Fig. 3). At the point Q, the prescribed displacement $u_n^* = 1\,mm$ at $x = 850$ mm is attained. Figure 6b presents the beam deflection for three values of force F_Q. The heights of punch pins at the start of calculation are assumed to be 50 mm. From the numerical solution the new heights are calculated by (68) and depicted in Fig. 7a.

The initial gaps at discrete points in Fig. 7b illustrate the effect of load values on punch profile at constant contact pressure. It is seen that the height differences become more significant at larger distance from the force F_Q application. The maximal height difference is less than 0.15 mm.

The distribution of contact tractions is presented in Fig. 8 for $F_Q = 5\,kN$. The maximum value is reached for the control function Hermite 2, the least value for $c(x) = const = 1$. In the latter case the contact force is the same at each pin: $P_j = 2.987\,kN$ and the punch load equals $F_0 = 14.935\,kN$. This means that the present design requires the considerably higher load to execute the control at the efficiency load factor $f_0 = \frac{F_0}{F_Q} = 2.987$. At other force levels $F_Q = 4\,kN$, $F_Q = 6\,kN$, the maximal contact forces ($c(x) = const = 1$) are $P_{j\max} = 2.41\,kN$, $P_{j\max} = 3.56\,kN$, respectively, and the external punch loads in these cases are $F_0 = 12.07\,kN$, $F_0 = 17.81\,kN$, corresponding to load factors $f_0 = 3.0$ and 2.987.

3.1.2 Model 2: continuous contact interaction

Consider now the continuous contact interaction for the elastic punch in the plane stress state. The punch interaction is performed in the segment $420 \le x \le 480$ ($L_1 = 420$, $L_4 = 480$), and its height is 50 mm (see Figure 2b). The uniform pressure distribution, $c(x) = 1$, was assumed in the numerical solution and the normal displacement $u_n^{(1)}(x, p_n)$ was calculated by the finite element method, using $p$version technique, cf. Szabó and Babuska (1991). The punch is loaded by pressure $p_n = p_{\max}$ at the contact boundary $z = 0$ and by the same pressure at the upper boundary for $z = 50$ mm. The elastic boundary value problem has been solved for differing finite element meshes ($n_x = 4, 8, 12$; $n_z = 5$, where n_x, n_z is number of elements in x and z directions) using polynomial order $3 \le p \le 8$ for quadrilateral finite elements with the shape functions in the trunk space. NDOF at $n_x = 4$, $n_z = 5$, $p = 3, 8$ is equal to 135, 735 at $n_x = 8$, $n_z = 5$, $p = 3, 8$ is 270, 1470. The normal displacement distribution on the boundary surfaces exhibits good convergence for increasing p. For $p \ge 6$, the numerical results differ very little for all meshes, their difference being smaller than 0.15%.

The contact conditions are checked at the Lobatto integral points. The discretized problem is solved in the following steps:

1. Calculation of the contact pressure by (6), and F_0 calculated by (3).
2. Calculation of the vertical beam displacement in contact zone from contact pressure and load F_Q (see (65b)) and (65c))
3. Calculation of the elastic displacement ($u_z^{(1)e}(x, z = 0) = -u_n^{(1)} = -u_n^{(1)}(p_n, F_0)$) in punch from a separate solution (see (70)).
4. From Signorini contact condition: $d = 0$, we can find initial gap ${}^{iter}g^{(0)}$ and rigid body displacement ${}^{iter}\lambda$ (see (72), (65c), (66).
5. As the initial gap modifies punch shape, the iteration process must be used. The steps 3 and 4 are continued until

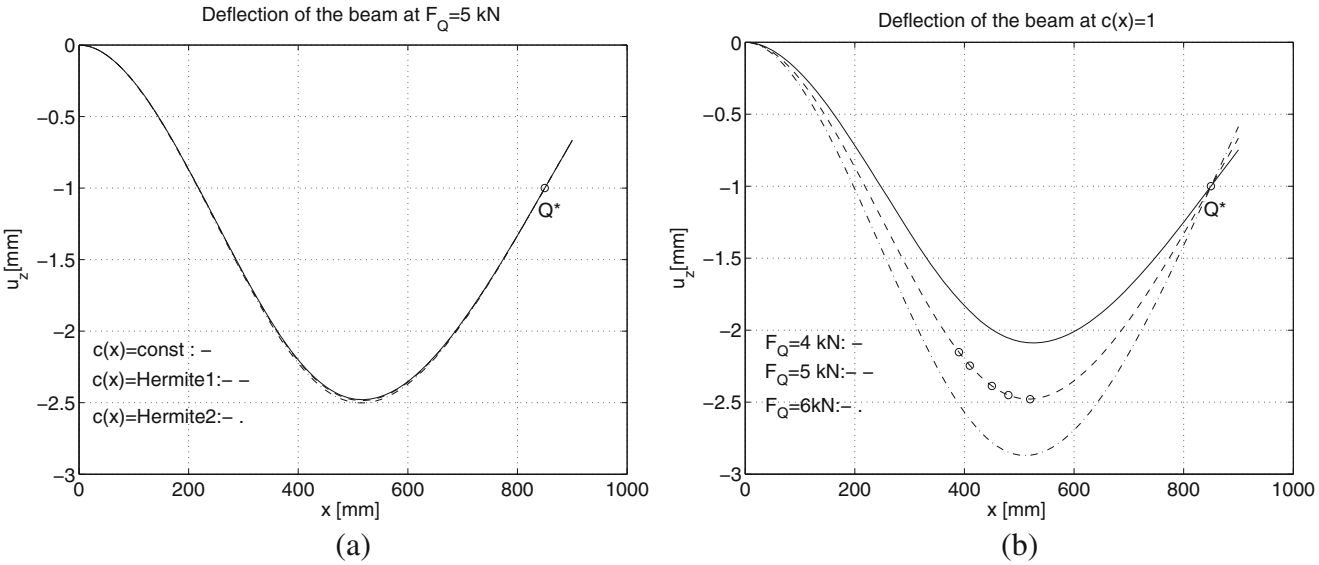

Fig. 6 Deflection of the beam at **a** $F_Q = 5000\,N$ for different control functions and **b** beam deflection for $c(x) = 1$; the prescribed forces are $F_Q = 4\,kN$, $F_Q = 5\,kN$, and $F_Q = 6\,kN$. Position of the punch is denoted by circles at $F_Q = 5\,kN$, see Fig. 6b

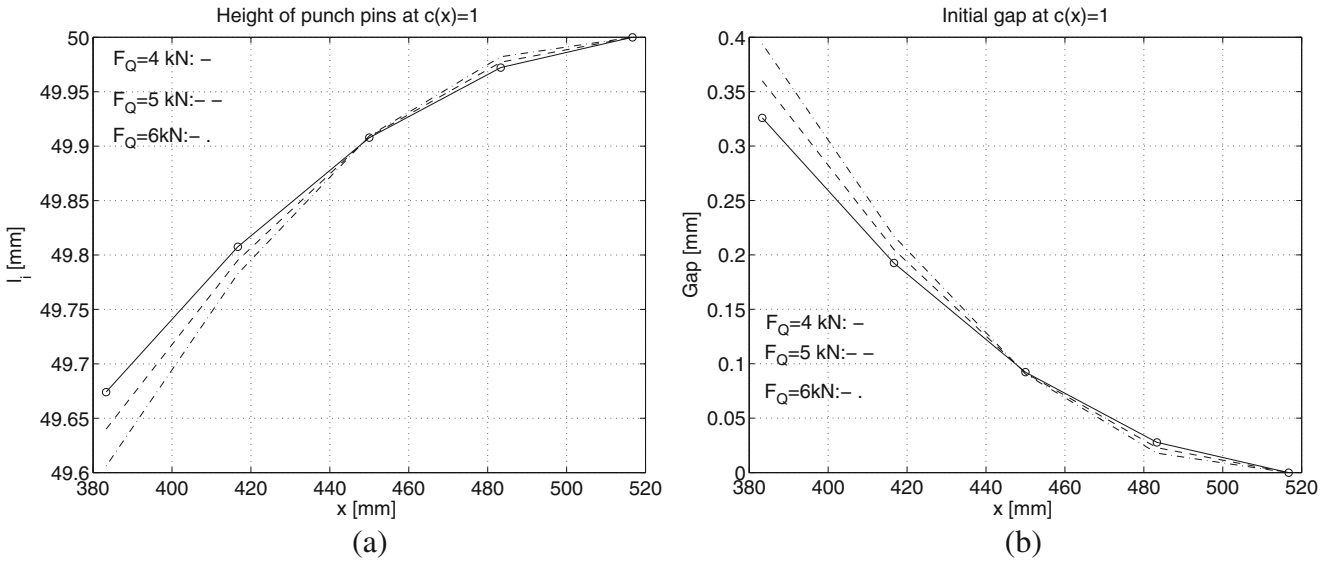

Fig. 7 **a** Heights of the punch pins. **b** Initial gaps between the punch pins and beam at different load values at $c(x) = 1$

the satisfactory convergence condition for shape modification is reached (cf. Páczelt et al. (2016)].

The rigid body vertical displacement of punch, $\lambda = \lambda_F^{(1)}$, is a displacement in the $-z$ direction at point $x = 420$, $z = 50$. In our case for $F_Q = 5\,kN$, the final value is $\lambda_F^{(1)} = 2.511$ mm. The deflection and initial gap are presented in Fig. 9a, b for all values of forces F_Q. For the optimal solution, the values the load F_0 and pressure $p_{\max}$ are collected in Table 1.

The beam deflection profiles for both discrete and continuous punch actions are very similar (see Figs. 6 and 9). Note that the contact zone for discrete punch action is much larger (300 mm), than that for continuous action (60 mm) at the same centre position $x = 450$ mm. The force efficiency factors in all cases are practically equal to 3.0.

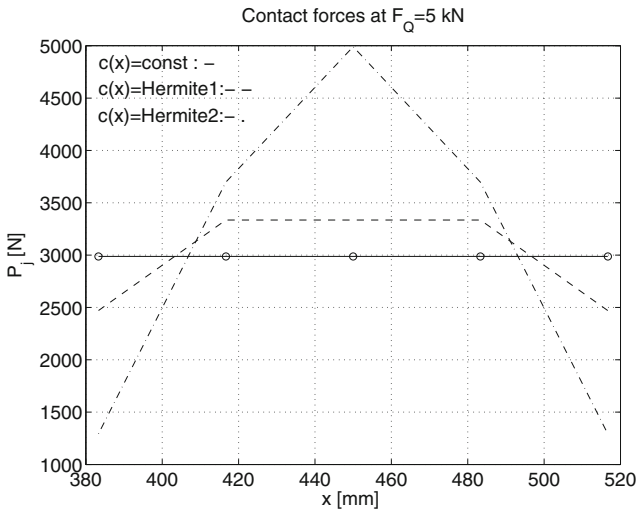

Fig. 8 Distribution of contact tractions at $F_Q = 5\,kN$

3.2 Example for the second variant: allowed beam support translation

In this case, the load equilibrium requires that $F_0 = F_Q$ (cf. Figure 4). In the first step, the rigid body displacement $\lambda_F^{(2)}$ is calculated from Eq. (11). From contact condition between beam and punch, the rigid body displacement $\lambda_F^{(1)}$ is determined from (18). Only several iterations are required to reach the solution. The beam deflection is shown in Fig. 10a. The punch pins profile is presented in Fig. 10b.

The force efficiency factor $f_0 = F_0/F_Q$ in this case is equal to 1. The rigid body punch and beam displacements are collected in Table 2 at different F_Q.

3.3 Example for 3rd variant: beam allowed for rigid body translation and rotation

Consider the beam of crosssection dimensions $a_b = 20$, $h_b = 75\,mm$ (cf. Fig. 5). In this case, the load on the punch is $F_0 = F_{Q_1} + F_{Q2}$, where $F_{Q_2} = (1-\zeta)F_{Q_1}$, $F_{Q_1} = 4, 5, 6\,kN$, and $\zeta = 0.5$. The prescribed vertical displacements at the points Q_1 *and* Q_2 are assumed: $u_{1n}^{\bullet} = 5$ *mm* and $u_{2n}^{\bullet} = 10\,mm$. Let us note that in the case of contact interaction at Q_1 and Q_2, the displacements are specified from the loadpenetration rules. The punch center coordinate is.

$$x_0 = \frac{x_{Q1} + x_{Q_2}(1-\zeta)}{2-\zeta} = 316.66\,mm, because x_{Q_1} = 50, x_{Q_2} = 850\,mm.$$

In the first step, the rigid body motion components $\lambda_F^{(2)}$ and $\lambda_M^{(2)}$ are calculated form (24).

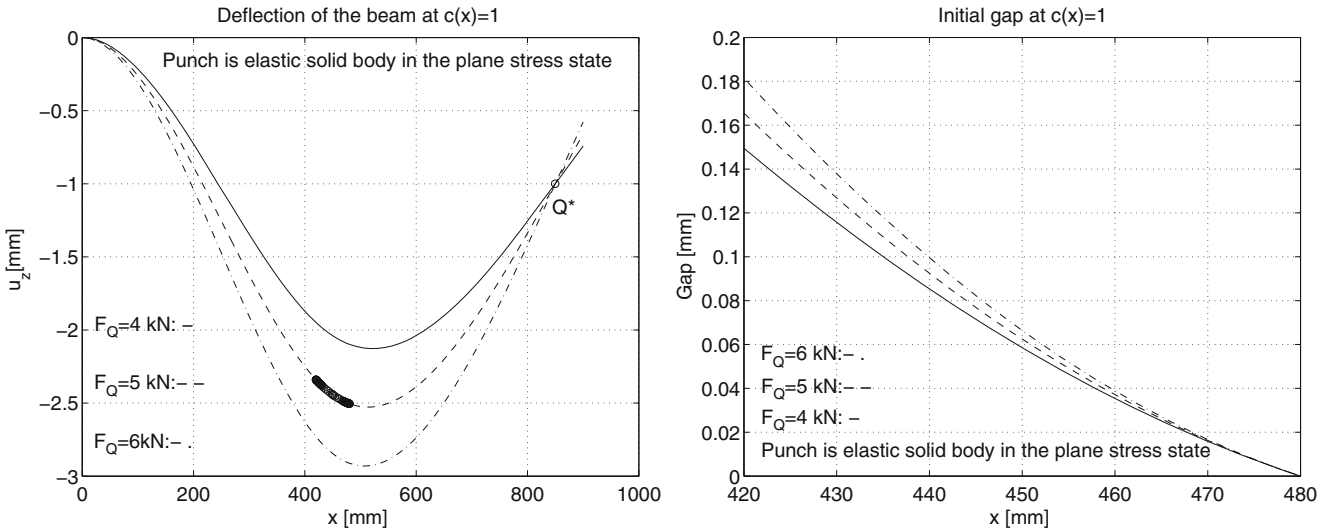

Fig. 9 Punch is an elastic solid body: **a** displacements of the beam interacting with punch contact surface (thick line, for punch action $F_Q = 5\ kN$) and **b** initial gap between punch and beam

From the contact condition between the punch and beam, the rigid body displacement $\lambda_F^{(1)}$ is easily determined in the several iterative steps, see (31). The deflection of the beam is shown in Fig. 11a. The heights of the punch pins constituting the contact gap are demonstrated in Fig. 11b. The punch vertical translation $\lambda_F^{(1)}$ and the loading force F_0 are therefore required for proper operation of gripper at the points Q_1 and Q_2. The rigid body displacements are collected in Table 3. Let us note that for varying control requirements at the contact points, the sliding or rotating punch can be applied assuring proper load F_0 position at each case.

4 Localized and distributed punch action: effect of design constraints

The numerical examples presented in Sect. 3 illustrate the discrete and continuous punch action in order to control the deflection at point Q (or at several points, as discussed in variant 3). In the design of such control system, the punch position x_0 and length $L_{1-4} = L_4 - L_1$ of the contact zone are important variables, as the applied load value and the maximal contact pressure should be minimized. Also, the maximal beam stress $\sigma_{\max}$ in the loaded state should not exceed the critical stress value, $\sigma_{\max} \le \sigma_u$. Assume first the contact pressure distribution as the design variable subject to optimization.

Table 1 Maximal contact pressures and punch loads for the optimal solution

$F_Q\,(kN)$	$F_0\,(kN)$	$p_{\max}\,(MPa)$
4	12.13	10.11
5	15.02	12.51
6	17.90	14.92

4.1 Contact pressure distribution: optimization for deflection control

Consider the cantilever beam under punch action on the contact zone $L_{1-4} = L_4 - L_1$ inducing the deflection $w_Q = -u_z$ at the location Q. Apply the unit force $F = 1$ at Q, inducing the state $M^{(q)}(x)$, $\kappa^{(q)}(x)$, $w^{(q)}(x)$ (bending moment, curvature, deflection) in the beam The independent punch action induces the state $M(x)$, $\kappa(x)$, and $w(x)$.

The virtual work equation is

$$Fw_Q = \int_0^L M^{(q)}\kappa\,dx = \int_0^L M\kappa^{(q)}dx = \int_{L_1}^{L_4} p_n w^{(q)} a_b dx \tag{32}$$

where $M = EI\kappa$, $M^{(q)} = EI\kappa^{(q)}$, and $M^{(q)}\kappa = EI\kappa^{(q)}\kappa = M\kappa^{(q)}$, p_n is the contact pressure between punch and beam, a_b is the beam crosssection width in direction y, h_b is the beam crosssection height in direction z, $I = a_b h_b^3/12$ inertia moment of the cross section, and E is the Young's modulus.

From (32), we have

$$w(x = x_Q) = w_Q = \int_{L_1}^{L_4} p_n w^{(q)} a_b dx \tag{33}$$

Now, several optimization problems can be stated

1. Contact force specified: maximize deflection w_Q

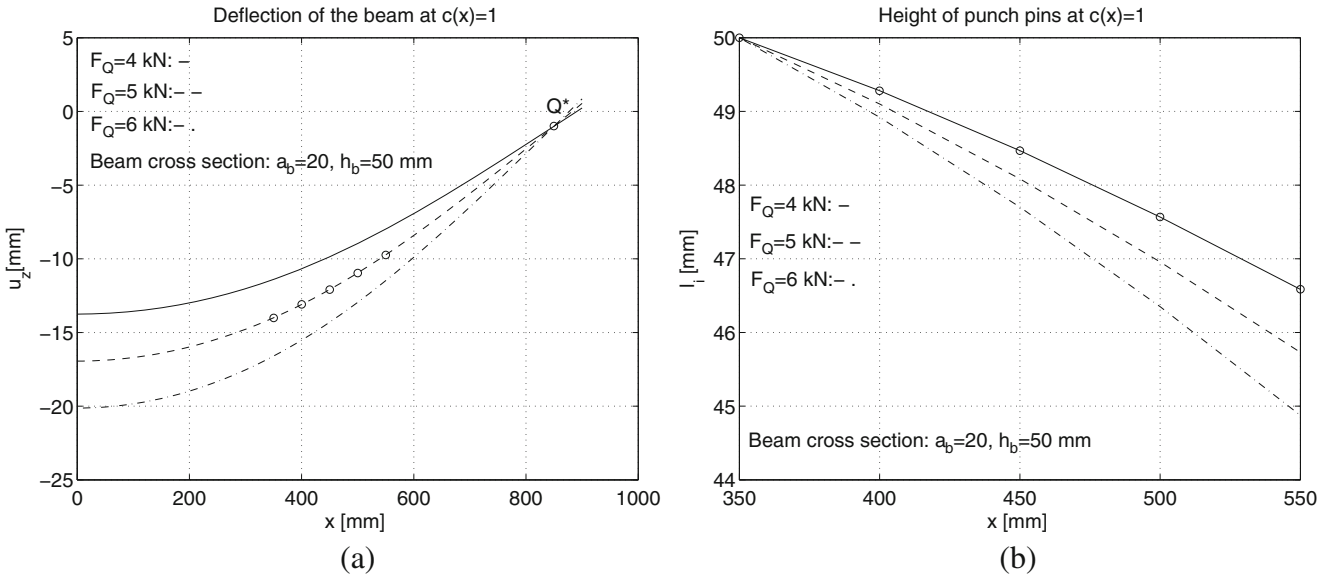

Fig. 10 Deflections of the beam (**a**) and heights of the punch pins/number of pins = 5 (**b**)

2. Deflection w_Q specified: minimize the punch force F_0
3. Deflection w_Q specified: minimize the maximal pressure $p_{\max}$

Problem 1:

$$\max \int_0^L M\kappa^{(q)} dx = \int_{L_1}^{L_4} p_n w^{(q)} a_b dx \quad subject\ to \quad \int_{L_1}^{L_4} p_n a_b\, dx - F_0 = 0 \tag{34}$$

Taking the functional

$$L_{p1} = \int_{L_1}^{L_4} p_n w^{(q)} a_b\, dx - \lambda \left(\int_{L_1}^{L_4} p_n a_b\, dx - F_0 \right) \tag{35}$$

its variation provides the stationary condition

$$\delta L_{p1} = \int_{L_1}^{L_4} \delta p_n \left(w^{(q)} - \lambda \right) a_b\, dx = 0, \quad that\ is \quad w^{(q)} = \lambda = const \tag{36}$$

It is seen that the problem formulation of optimal pressure distribution has no extremum, since the displacement $w^{(q)}$ is not constant, but λ is assumed constant. There is only the singular optimal solution for the concentrated contact force action located at $w_{Q\max}$ in the contact zone.

Table 2 Punch and beam rigid body displacements and maximal contact pressures for second variant: $a_b = 20$, $h_b = 50\,mm$

$F_Q\,(kN)$	$\lambda_F^{(1)}, \lambda_F^{(2)}$ (mm)	$p_{\max}\,(MPa)$
4	11.402, 13.752	8.0
5	14.003, 16.940	10.0
6	16.603, 20.128	12.0

Problem 2:

The same result as for problem 1.

Problem 3:

Assume the penalty approach and the contact pressure functional

$$I_{p3} = \int_{L_1}^{L_4} \left(\frac{p_n}{p_0} \right)^m a_b\, dx, m > 1 \tag{37}$$

where p_0 is the reference pressure, $p_0 \approx p_{\max}$, and $p_0 \le p_{\max}$.

Then

$$L_{p3} = \int_{L_1}^{L_4} \left(\frac{p_n}{p_0} \right)^m a_b\, dx - \lambda \left[\int_{L_1}^{L_4} p_n w^{(q)} a_b\, dx - w_Q \right] \tag{38}$$

The variation of L_{p3} has the following form

$$\delta L_{p3} = \int_{L_1}^{L_4} \left\{ m \left(\frac{p_n}{p_0} \right)^{m-1} - \lambda w^{(q)} \right\} \delta p_n\, a_b\, dx = 0 \tag{39}$$

and the stationary conditions are as follows

$$p_n = \lambda^* \left(w^{(q)} \right)^{\frac{1}{m-1}} \quad where \quad \lambda^* = \left(\frac{\lambda p_0^m}{m} \right)^{\frac{1}{m-1}} \tag{40}$$

The value of λ^* is specified from the equality $w_Q^0 = \int_{L_1}^{L_4} p_n w^{(q)} a_b dx$.

Consider now the case of symmetric pressure distribution relative to the contact zone center, assuming that

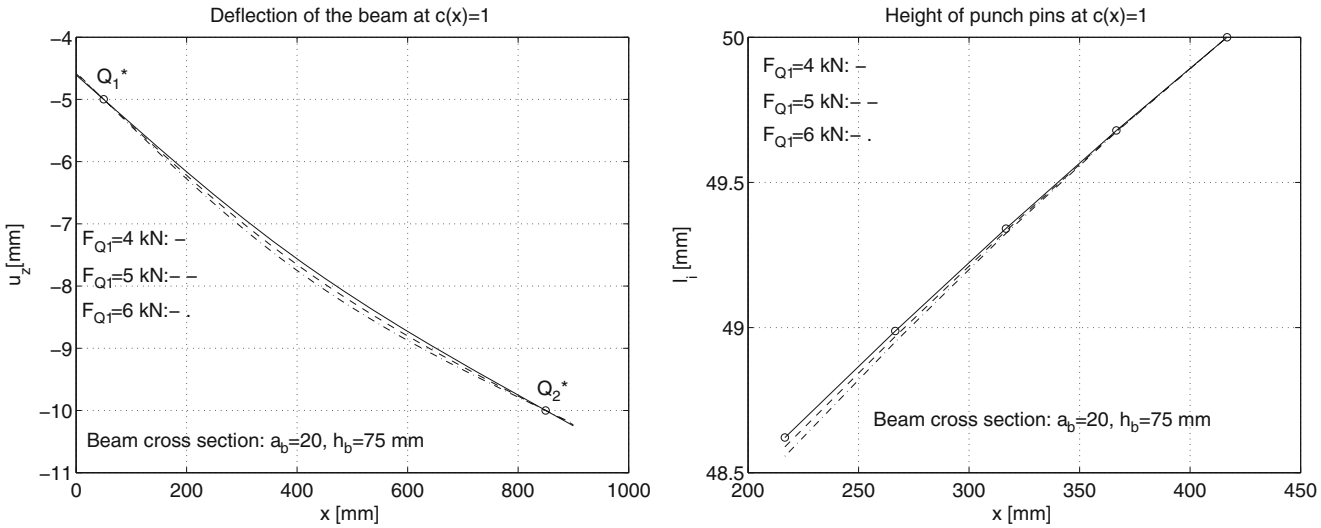

Fig. 11 Deflections of the beam **a** and heights of the punch pins **b** for the solution of variant 3 (see Fig. 5)

$$p_n\left(L_1+\bar{\xi}\right)=p_n\left(L_4-\bar{\xi}\right) \tag{41}$$

where $\bar{\xi}$ specifies the position of two symmetrically located points.

The virtual work relation now is

$$\begin{aligned}\int_0^L M\kappa^{(q)}dx &= \int_{L_1}^{L_4} p_n w^{(q)} a_b dx \\ &= \int_0^{(L_4-L_1)/2} p_n\left(L_1+\bar{\xi}\right)\frac{w^{(q)}\left(L_1+\bar{\xi}\right)+w^{(q)}\left(L_4-\bar{\xi}\right)}{2}a_b\,d\bar{\xi}\end{aligned} \tag{42}$$

Denote

$$\tilde{w}^{(q)}\left(\bar{\xi}\right)=\frac{w^{(q)}\left(L_1+\bar{\xi}\right)+w^{(q)}\left(L_4-\bar{\xi}\right)}{2} \tag{43}$$

then we have

$$\int_0^L M\kappa^{(q)}dx=\int_0^{(L_4-L_1)/2} p_n\left(L_1+\bar{\xi}\right)\tilde{w}^{(q)}a_b\,d\bar{\xi} \tag{44}$$

and from (40), there is

$$p_n=\lambda^*\left(\tilde{w}^{(q)}\right)^{\frac{1}{m-1}} \tag{45}$$

The analysis presented characterizes the optimal contact pressure distribution. Figure 12 presents the optimal pressure distribution for varying value of the exponent m and minimization of the functional I_{p3}. It is seen that for $m=4$, the pressure tends to the uniform distribution for both unconstrained and symmetry constrained cases. If there is no constraint set on the maximal pressure value, then the concentrated load action is optimal. Its value and position are determined by requiring the deflection $u_z=-u_n^*$ at Q and accounting for the beam stress constraint $\sigma_{\max}\le\sigma_u$. When the distributed punch action is considered, and the integral constraint is set on the contact pressure, then its distribution is uniform on the whole contact zone. The required punch load for specified deflection $u_z=-u_n^*$ will then be higher from the concentrated load value.

4.2 Concentrated and distributed cantilever beam control

Referring to Fig. 2, consider the cantilever beam under the action of concentrated load F_Q and the punch action is

Table 3 The maximal contact pressure and rigid body displacements resulting from solution of variant 3

$F_0=F_{Q_1}+F_{Q_2}$ $F_{Q_1}, F_{Q_2}\,(kN)$	$\lambda_F^{(1)},\ \lambda_F^{(2)},\ \lambda_M^{(2)}\cdot 10^3$ (mm, mm, rad)	$p_{\max}\,(MPa)$
4.0, 2.0	7.671, 4.612, 7.86	12.0
5.0, 2.5	7.765, 4.586, 8.26	15.0
6.0, 3.0	7.860, 4.566, 8.67	18.0

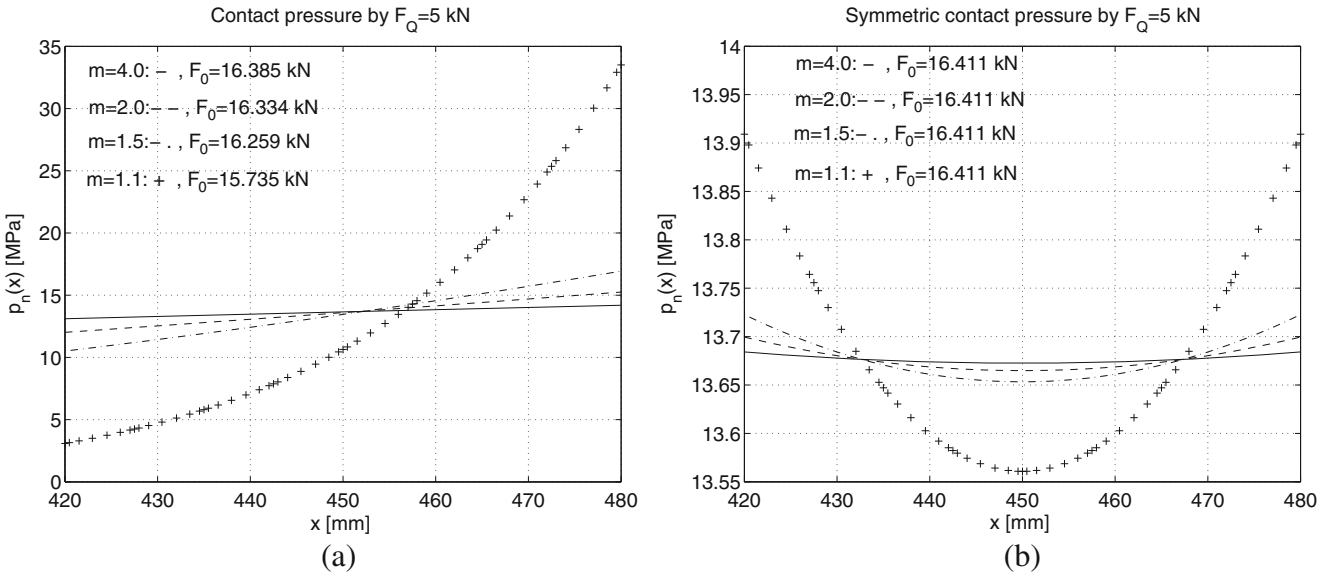

Fig. 12 Contact pressure distribution obtained from the optimization procedure: **a** unconstrained distribution and **b** symmetry constrained distribution

simulated by the concentrated load F_0. Assume first that the load positions satisfy the inequality $x_0 \le x_Q$. The bending moment in the beam is expressed as follows

$$M = M_b + (F_Q - F_0)x \qquad 0 \le x \le x_0, \quad M = -F_Q(x_Q - x) \qquad x_0 \le x \le x_Q \tag{46}$$

where $M_b = -F_Q x_Q + F_0 x_0$ is the boundary moment.

The normal deflection at the point Q (along—$z$axis) due to force F_Q (can be expressed from the formulae of Appendix 3) equals

$$w_Q = -\frac{F_Q}{3EI} x_Q^3 \tag{47}$$

The deflection w_Q^0 at Q due to load F_0 is

$$w_Q^0 = \frac{F_0}{3EI}\left(\frac{3}{2}x_Q x_0^2 - \frac{1}{2}x_0^3\right) \tag{48}$$

Introducing the nondimensional variables

$$\frac{F_0}{F_Q} = f_0, \quad \frac{x_0}{x_Q} = \xi, \quad \frac{M_b}{F_Q x_Q} = \tilde{M}_b = -1 + f_0\xi, \quad \frac{w_t}{|w_Q|} = \tilde{w}_t \tag{49}$$

Now, we can express the total deflection $w_t = w_Q + w_Q^0$ at Q as follows

$$\tilde{w}_t = -1 + \frac{1}{2}(3\xi^2 - \xi^3) f_0 \quad \text{for } \xi \le 1 \tag{50}$$

For the load F_0 acting on the right side of Q, $x_Q \le x_0$, the total deflection at Q equals

$$w_Q^0 = \frac{F_0}{3EI}\left(\frac{3}{2}x_Q^2 x_0 - \frac{1}{2}x_Q^3\right), \quad w_Q = -\frac{F_Q}{3EI}x_Q^3 = -|w_Q|, \quad \tilde{w}_t = -1 + \frac{1}{2}(3\xi - 1)f_0 \quad \text{for } \xi \ge 1 \tag{51}$$

For specified $\tilde{w}_t$, the required value of load F_0 is expressed as follows

$$f_0^- = \frac{F_0}{F_Q} = \frac{2\left(1 + \tilde{w}_t\right)}{3\xi^2 - \xi^3} \quad \text{for } \xi \le 1 \qquad f_0^+ = \frac{F_0}{F_Q} = \frac{2\left(1 + \tilde{w}_t\right)}{3\xi - 1} \quad \text{for } \xi \ge 1 \tag{52}$$

At $\tilde{w}_t = 0$ and $w_Q^0 + w_Q = 0$, this means that there is no interaction of gripper with the assembled element. For contact interaction, the relative penetration depth equals $\delta = w_t$ and $|w_Q| < w_Q^0$. The diagrams $f_0(\xi)$ for positive values of $\delta = w_t > 0$ can be plotted. The region above the curve for $\tilde{w}_t = 0$ (see Fig. 13) corresponds to contact interaction. The load efficiency factor $f_0 = F_0/F_Q$ strongly depends on the punch load F_0 position. Usually, the value of $\xi = x_0/x_Q$ is selected in a specific design case with account for contact pressure and beam strength constraints. For instance, assume the punch load to belong to segments $0.4 \le \xi \le 0.7$ or $1.2 \le \xi \le 1.5$. Then the point $\xi = 450/850 = 0.529$, $f_0 \approx 3$, marked in Fig. 13 (point B) represents the design discussed in Sect. 3.1, cf. (Fig. 9), for $F_Q = 5\,kN$, $w_t = u_n^* = 1\,mm$, $|w_Q| = |u_{n,load}^{(2)}| = 24.56\,mm$, and $\tilde{w}_t \approx 0.04$.

Consider the strength constraint. The critical bending moment results from the stress constraint $M \le M_c = a_b h_b^2 \sigma_u / 6$, where σ_u is the ultimate stress. Denoting $\tilde{M} = M/(F_Q x_Q)$, the maximal bending moment for $\xi \le 1$ is reached at the support $x = 0$ and its absolute value equals

$$|\tilde{M}_b| = -1 + f_0\xi \tag{53}$$

For $\xi \ge 1$, the maximal bending moment is reached at Q and its absolute value is

$$|\tilde{M}_Q| = f_0(\xi-1) \tag{54}$$

Satisfying the strength conditions $|\tilde{M}_b| \le \tilde{M}_c$ and $|\tilde{M}_Q| \le \tilde{M}_c$, in view of (52), (53), and (54), the limits of applicable load positions are expressed by the inequalities

$$\xi \ge \xi_c^- = \frac{1}{2}\left[3-\sqrt{9-8\beta}\right] \quad where \quad \beta = \frac{1+\tilde{w}_t}{1+\tilde{M}_c} \tag{55}$$

$$\xi \le \xi_c^+ = \frac{2\overline{\beta}-1}{2\overline{\beta}-3} \quad where \quad \overline{\beta} = \frac{1+\tilde{w}_t}{\tilde{M}_c} \tag{56}$$

Figure 13 shows the admissible segment of punch action satisfying the constraints (55) and (56). Calculated values are $\xi_c^- = 0.5012$, $f_0^- = 3.31$, $\xi_c^+ = 14.76$, and $f_0^+ = 0.048$. At another beam cross section $a_b = 20$, $h_b = 75\ mm$, there are $\xi_c^- = 0.5613$, $f_0^- = 2.96$, $\xi_c^+ = 5.572$, and $f_0^+ = 0.144$. For the distributed punch action, the contact zone length parameter $\tilde{L}_{1-4} = L_{1-4}/x_Q = (L_4 - L_1)/x_Q$ affects the resultant punch load relative to the concentrated load action at the same position. The required punch load value is higher for the same value of induced displacement $\tilde{w}_t$.

4.3 Translating beam control under concentrated loads, variant 2

Consider the beam of Fig. 4 with the sliding support at the left end, loaded by the concentrated load $F_0 = F_Q$ at the distance x_0 and the specified contact force F_Q at Q located at the distance x_Q.

Consider first the case $x_0 \le x_Q$ or $\xi \le 1$. At the support, the transverse force equals $F_b = 0$ and the moment is $|\tilde{M}_b| = 1 - f_0\xi$. The deflection form now is expressed as follows

$$w = -\frac{F_Q}{2EI}(x_Q - x_0)x^2 + w_b, \quad 0 \le x \le x_0,$$
$$w = -\frac{F_Q}{2EI}\left[(x_Q x - x_0^2)x + \frac{1}{3}(x_0^3 - x^3)\right] + w_b, \quad x_0 \le x \le x_Q \tag{57}$$

For $x_0 \ge x_Q$ or $\xi \ge 1$, we have

$$w = \frac{F_Q}{2EI}(x_0 - x_Q)x^2 + w_b, \quad 0 \le x \le x_Q,$$
$$w = \frac{F_Q}{2EI}\left[\left(x_0 x - x_Q^2\right)x - \frac{1}{3}\left(x^3 - x_Q^3\right)\right] + w_b, \quad x_Q \le x \le x_0 \tag{58}$$

where $w_b = \lambda_F^{(2)}$ denotes the beam translation at the support. Requiring $w = w_t$ at Q, the beam translation w_b is determined, thus

$$\tilde{w}_b = \tilde{\lambda}_F^{(2)} = \tilde{w}_t + 1 - \frac{1}{2}(3\xi^2 - \xi^3), \quad \xi \le 1 \quad \text{and} \quad \tilde{w}_b = \tilde{\lambda}_F^{(2)} = \tilde{w}_t - \frac{3}{2}(\xi - 1), \quad \xi \ge 1 \tag{59}$$

where

$$\tilde{w}_b = \tilde{\lambda}_F^{(2)} = \frac{\lambda_F^{(2)}}{|w_Q|} = \lambda_F^{(2)}\frac{3IE}{F_Q x_Q^3}, \quad \tilde{w}_t = \frac{w_t}{|w_Q|}. \tag{60}$$

The diagram $\tilde{w}_b = \tilde{\lambda} = \lambda_F^{(2)}(\tilde{w}_t, \xi)$ can easily be constructed, see Fig. 14. It is seen that the sliding displacement changes sign at $\xi = 1$.

The present sliding support case differs essentially from the previous builtin case. The applied punch force is constant and does not depend on the position, but the deflection form radically changes when passing from $\xi \le 1$ to $\xi \ge 1$. Figure 15 presents both deflection forms for concentrated (Fig. 15a, b)

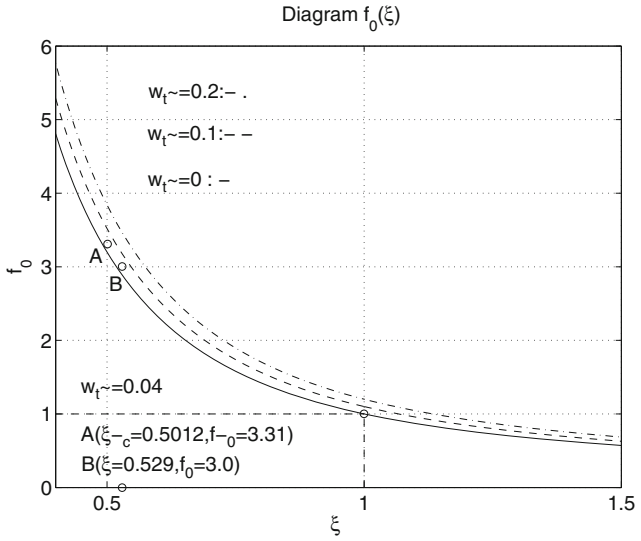

Fig. 13 Diagram $f_0 - \xi$ of punch load dependence on its position for fixed deflection $\tilde{w}_t$ at the contact point interaction Q. The strength constraints $\xi_c^- \le \xi \le \xi_c^+$ provide the admissible segment for punch action. Beam cross section $a_b = 20$, $h_b = 50\ mm$, $\xi_c^- = 0.5012$, and $\xi_c^+ = 14.76$

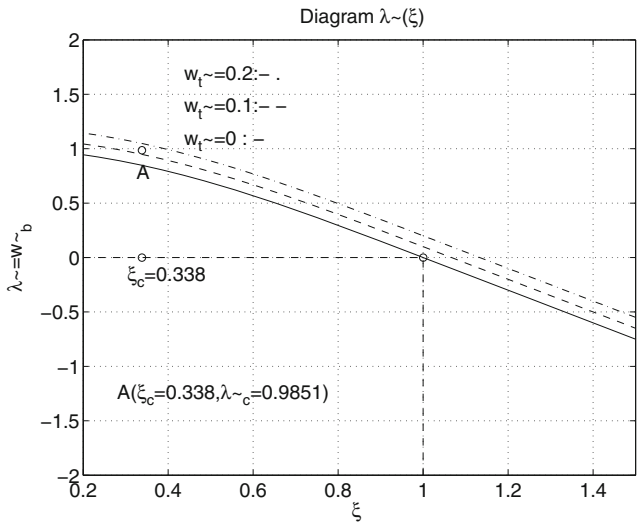

Fig. 14 Diagram for $\tilde{\lambda} = \tilde{\lambda}_F^{(2)}(\tilde{w}_t, \xi)$. (Beam cross-section sides are $a_b = 20$, $h_b = 75\ mm$)

and distributed (Fig. 15c) punch action. The present case is convenient for more precise control at Q by requiring both deflection and slope to be kept at specified values and allowing for sliding punch action. In Fig. 15a, c the solutions of the optimization problems satisfying stress constraint are presented. In Fig. 15 the optimal solution point is marked by o.

5 Concluding remarks

The optimal design of punch action in order to control normal displacement at a loaded boundary point in a structural element has been discussed in the paper and illustrated by the specific examples of beam deflection control. It was demonstrated that the support constraint can affect essentially the punch load and the beam deflected form. This new class of problems is characterized by a set of design variables, such as contact pressure distribution $p_n(x)$, punch resultant load F_0, punch centre position x_0, and the size of contact zone L_{1-4}. The minimization of punch load or the maximal contact pressure, required for displacement control, has been discussed, also the effect of punch position and contact zone size on the punch load value was considered.

The present problem formulation can be extended to more advanced control problems. First, for the gripper operation requiring varying load and displacement control at Q, or following the loading path $F_0 = F_0(u_n^*)$, the punch action should be executed for properly varying load F_0. The other

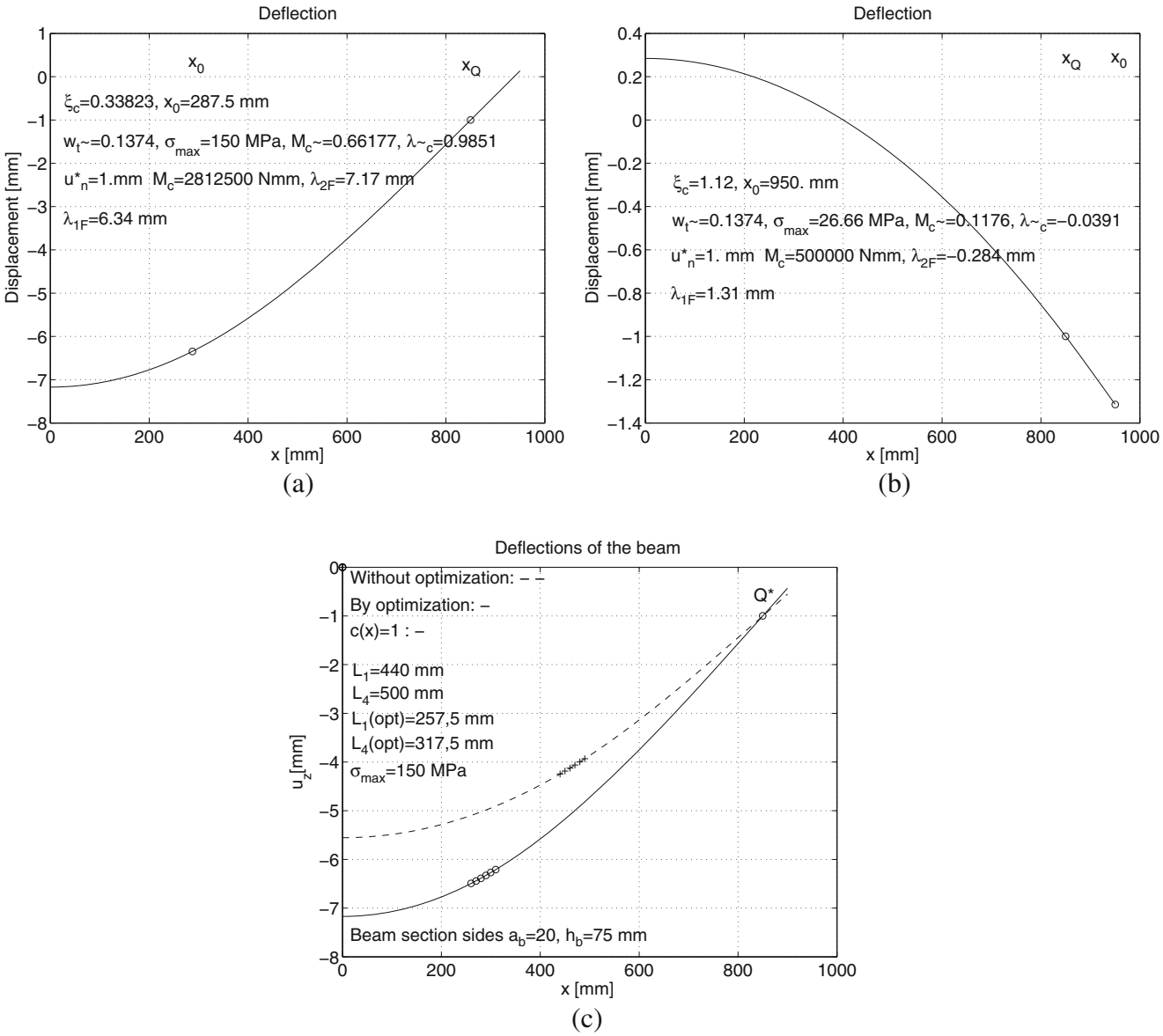

Fig. 15 Beam deflection forms: **a** for $\xi \leq 1$, **b** for $\xi \geq 1$, and **c** for distributed punch action at $\xi \leq 1$ (beam cross-section sides: $a_b = 20, \quad h_b = 75\,mm$, $\tilde{\lambda_c} = \lambda_F^{(2)}$)

extension is related to control of both the deflection and its slope at Q. Such control can be performed by varying loads of two punches. Applying such punch action to plate elements, the normal displacement and the orientation angles of the normal vector to the deflected surface at Q can be controlled. Any tool attached transversely at Q to the plate could then execute both normal and inplane displacements. Such advanced control problems will be discussed in a separate paper.

6 Replication of results

The computer codes are written in FORTRAN and MATLAB in the research form. To use them without additional comments could be complicated. If anybody is interested in the programs, please write to István Páczelt.

Acknowledgments The present research was partially supported by the Hungarian Academy of Sciences, by the grant National Research, Development and Innovation Office—NKFIH: K115701.

Funding Information Open access funding provided by University of Miskolc (ME).

Compliance with ethical standards

Conflict of interest The authors declare that they have no conflict of interest.

Appendix 1

The starting point of numerical analysis is related to discretization of (7)

$$d = \left(u_n^{(2)}(p_n) + u_{n,load}^{(2)}\right) - \left(u_n^{(1)}(p_n) + \lambda\right) + g^{(0)} = 0$$

The displacements induced by the contact tractions are

$$u_n^{(\alpha)}(p_n) = u_n^{(\alpha)}(x, p_n) \Rightarrow u_n^{(\alpha)}(x_i, P_j) = \sum_{j=1}^{kont} H^{(\alpha)}(x_i, s_j) P_j, \quad x_i, i = 1, \ldots, kont, \quad \alpha = 1, 2 \tag{62a}$$

and from the given load F_Q, the displacement of body 2 is

$$u_{n,load}^{(2)}(x) \Rightarrow u_{n,load}^{(2)}(x_i), i = 1, \ldots, kont \tag{62b}$$

Introduce the vectors (contact force, displacement from F_Q, initial gap).

$$\mathbf{p}^T = [P_1 \ldots P_j \ldots P_{kont}]^T, \quad \mathbf{u}_{n,load}^{(2)T} = \left[u_1^{(2)} \ldots u_i^{(2)} \ldots u_{load}^{(2)}\right]_{n,load}^T,$$

$$\mathbf{g}^{(0)T} = \left[g_1^{(0)} \ldots g_i^{(0)} \ldots g_{kont}^{(0)}\right]^T.$$

Next the vector $\mathbf{e}$ and the gap $\mathbf{d}$ after deformation are

$$\mathbf{e}^T = [1 \ldots 1 \ldots 1]^T, \quad \mathbf{d}^T = [d_1 \ldots d_i \ldots d_{kont}]^T \tag{63}$$

the influence matrices are

$${}^{(iter)}\mathbf{H} = {}^{(iter)}\mathbf{H}^{(1)} + {}^{(iter)}\mathbf{H}^{(2)} \tag{64}$$

the discretized gap after deformation can be written in the following form

$$\mathbf{d} = {}^{(iter)}\mathbf{H}\mathbf{p} + \mathbf{u}_{n,load}^{(2)} + {}^{(iter)}\mathbf{g}^{(0)} - \mathbf{e}^{(iter)}\lambda \tag{65a}$$

The displacements due to contact tractions are

$${}^{(iter)}\mathbf{g}^{(0)*} = {}^{(iter)}\mathbf{H}\mathbf{p} \tag{65b}$$

and from (65a) we get

$${}^{(iter)}\mathbf{g}^{(0)*} = -\mathbf{u}_{n,load}^{(2)} - {}^{(iter)}\mathbf{g}^{(0)} + \mathbf{e}^{(iter)}\lambda \tag{65c}$$

In this equation ${}^{(iter)}\mathbf{g}^{(0)}$, ${}^{(iter)}\lambda$are unknown. Assume that ${}^{(iter)}g_{j\min}^{(0)*} = \min {}^{(iter)}\mathbf{g}^{(0)*}$, that is minimum value is obtained at the $j$min component. Choosing the initial gap ${}^{(iter)}g_{j\min}^{(0)} = 0$, that is at the point $j = j$min, the initial gap is assumed to vanish.

Then, according to (65c) for $j$min component we get

$${}^{(iter)}\lambda = {}^{(iter)}g_{j\min}^{(0)*} + {}^{(iter)}u_{n,load;j\min}^{(0)} \tag{66}$$

After calculation of ${}^{(iter)}\lambda$, the gap vector is (see (65c))

$${}^{(iter)}\mathbf{g}^{(0)} = -\mathbf{u}_{n,load}^{(2)} - {}^{(iter)}\mathbf{g}^{(0)*} + \mathbf{e}^{(iter)}\lambda \tag{67}$$

The lengths of punch pins are

$$l_i = l_i^{(0)} - {}^{(iter)}\,g_i^{(0)}, i = 1, \ldots, kont \tag{68}$$

and the influence matrix element is

$${}^{(iter)}H_{i,i}^{(1)} = \frac{{}^{(iter)}l_i}{AE} \tag{69}$$

where A *and* E denote the crosssection area and Young's modulus. Usually, the convergent solution is obtained in the fast iterative process.

Appendix 2

Consider now the case, when the punch (body 1) deforms elastically in the plane stress state. In this case the discretisation is performed by the finite element technique. The control of contact conditions is made at the Lobatto integral points (Páczelt et al. 2015, 2016). The force F_0 and the contact pressure $p_n(x)$ are assumed as given. The value of $p_{\max}$ is obtained from the equilibrium equation, cf. (3). The punch displacement is assumed to be composed of a rigid body translation λ and an elastic translation $u_z^{(1)e} = u_n^{(1)}(p_n, F_0)$ reaching its value $\lambda + u_z^{(1)e}$ on the

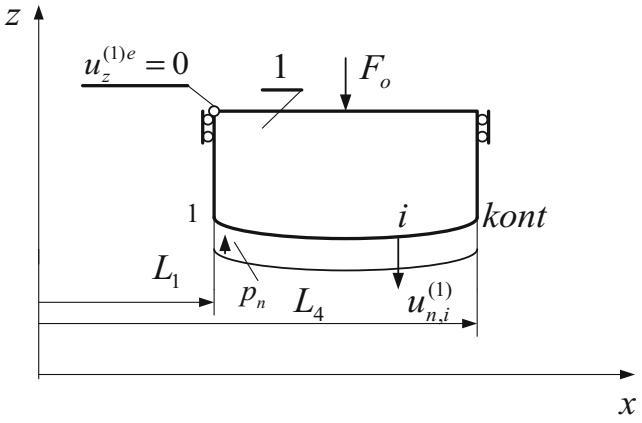

Fig. 16 Punch with its load F_0 and contact pressure $p_n(x)$: elastic displacement constraint $u_z^{(1)e}=0$

contact surface. For calculation of this normal elastic displacement $u_z^{(1)e}(x,z=0)=-u_n^{(1)}(p_n,F_0)$, the elastic boundary value problem is solved with the condition $u_z^{(1)e}=0$ at the upper punch boundary point, Fig. 16. Discretizing the elastic problem by finite element technique, we get the normal displacement $u_n^{(1)}$ on the contact surface. Between the punch (body 1) and the beam (body 2) the initial gap $g^{(0)}$ results from the punch contact surface shape. The geometrical contact condition is

$$d=\left(u_n^{(2)}(p_n)+u_{n,iload}^{(2)}\right)-\left(u_n^{(1)}(p_n,F_0)+\lambda\right)+g^{(0)}=0 \qquad (70)$$

After discretization, using the earlier defined influence matrix $\mathbf{H}^{(2)}$, the initial gap vector $\mathbf{g}^{(0)}$ is specified. As the initial gap changes in consecutive iterations, the discretized equation has the following form

$$\mathbf{d}=\mathbf{H}^{(2)}\mathbf{p}-{}^{(iter)}\mathbf{u}_n^{(1)}+\mathbf{u}_{n,load}^{(2)}+{}^{(iter)}\mathbf{g}^{(0)}-\mathbf{e}^{(iter)}\lambda=\mathbf{0}. \qquad (71)$$

After definition

$${}^{(iter)}\mathbf{g}^{0*}=\mathbf{H}^{(2)}\mathbf{p}-{}^{(iter)}\mathbf{u}_n^{(1)} \qquad (72)$$

the steps (65c)–(67) should be repeated.

Appendix 3

Using Betti theorem, the influence (Green) function for cantilever beam (Fig. 17) has the form.

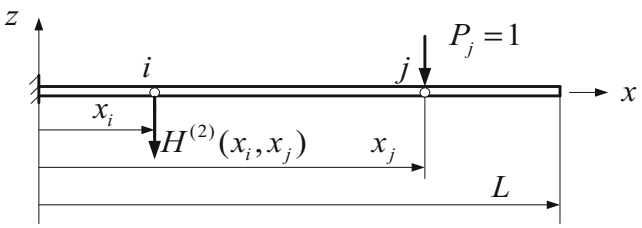

Fig. 17 Load for calculation of the Influence function of the cantilever beam

$$H^{(2)}(x_i,x_j)=H_{i,j}^{(2)}=\frac{1}{6EI}\left\{\left(3x_jx_i^2-x_i^3\right)+\langle x_i-x_j\rangle^3\right\},$$

where $\langle x_i-x_j\rangle^3=\begin{cases}(x_i-x_j)^3, & if\ x_i>x_j\\ 0, & if\ x_i\le x_j\end{cases}$, I is the inertia moment of cross section, and E is the Young's modulus.

References

Banichuk NV (2011) Introduction to optimization of structures. SpringerVerlag, London

Banichuk NV, Neittaanmaki PJ (2010) Structural optimization with uncertainties. Solid mechanics and its applications, vol 162. SpringerVerlag, Berlin

Goryacheva IG (1998) Contact mechanics in tribology. Kluwer Academic Publishers, Dordrecht

Konyukhov A, Schweizerhof K (2013) Computational contact mechanics. SpringerVerlag, Berlin

Li W, Li Q, Steven GP (2003) An evolutionary shape optimization procedure for contact problems in mechanical designs. Proc Inst Mech Eng C J Mech Eng Sci 217. https://doi.org/10.1243/095440603321509711

Monkman G, Hesse S, Steinmann R, Schunk H (2006) Robot grippers. WileyVCH, Berlin

Páczelt I (2000) Iterative methods for solution of contact optimization problems. Arch Mech 52:685–671

Páczelt I, Baksa A (2002) Examination of contact optimization and wearing problems. J Comput Appl Mech 3:61–84

Páczelt I, Szabó T (1994) Optimal shape design for contact problems. Structural optimization 7:66–75

Páczelt I, Baksa A, Szabó T (2007) Product design using a contactoptimization technique. Stroj VestnJ Mech E 53:442–461

Páczelt I, Mróz Z, Baksa A (2015) Analysis of steady wear processes for periodic sliding. J Comput Appl Mech 10:231–268

Páczelt I, Baksa A, Mróz Z (2016) Contact optimization problems for stationary and sliding conditions. In: Neittaanmaki P et al (eds) Mathematical modelling and optimization of complex structures, computational methods in applied sciences 40. Springer International Publishing, Cham, pp 281–312. https://doi.org/10.1007/9783319235646_16

Szabó B, Babuska I (1991) Finite element analysis. WileyIntersience, New York

Wriggers P (2002) Computational contact mechanics. Wiley, New York

Zabaras N, Bao Y, Srikanth A, Frazier WG (2000) A continuum Lagrangian sensitivity analysis for metal forming processes with applications to die design problems. Int J Numer Methods Eng 48(5):679–720